

Simple fermionic dark matter models and Higgs boson couplings

Nobuchika Okada^a and Toshifumi Yamada^b

^a *Department of Physics and Astronomy, University of Alabama,
Tuscaloosa, Alabama 35487, USA*

^b *Department of Physics, University of Tokyo,
7-3-1 Bunkyo, Tokyo 113-0033, Japan*

Abstract

We consider a simple extension of the Standard Model (SM) that incorporates a Majorana fermion dark matter and a charged scalar particle with a coupling to the SM leptons through renormalizable terms. Another renormalizable term involving the charged scalar and the Higgs boson gives rise to interactions between the dark matter and SM quarks at the one-loop level, which induce the elastic scatterings between dark matter and nucleus. The same term also affects the effective coupling of the Higgs boson to diphoton through a one-loop diagram with the charged scalar. Therefore, our model predicts a correlation between the spin-independent cross section for dark matter-nucleus elastic scatterings and a new contribution to the effective Higgs boson coupling to diphoton. When the spin-dependent cross section is large enough to be tested in future direct dark matter detection experiments, the Higgs-diphoton decay rate shows a sizable deviation from the SM prediction. We also consider the case where the fermion dark matter is a Dirac particle. Most of discussions is similar to the Majorana case, but we find that the magnetic dipole moment of the Dirac fermion dark matter is loop-induced and this interaction dominates the spin-independent cross section for dark matter-nucleus elastic scatterings. We find that the resultant cross section is about an order of magnitude below the current experimental bound and hence can be tested in the near future.

1 Introduction

The Wilkinson Microwave Anisotropy Probe (WMAP) observations [1] have established the existence of cold, non-baryonic dark matter (DM), whose abundance is measured to be

$$\Omega_{\text{DM}}h^2 = 0.112 \pm 0.006 . \quad (1)$$

Since a DM candidate is missing in the standard model (SM), its existence motivates us to consider physics beyond the SM. One notable fact about this measured DM abundance is its possible relation to physics at the TeV scale. Let us assume that the DM particle is a weakly-interacting massive particle (WIMP) that has been in thermal equilibrium with SM particles and decouples from the thermal bath when the temperature drops below its mass scale, *i.e.*, the DM particle is assumed to be a cold relic. The measured DM abundance, Eq. (1), then implies that the thermally averaged cross section times velocity for DM annihilations to SM particles at the time of decoupling satisfies

$$\langle\sigma v\rangle_{t_{\text{dec}}} \sim \frac{g^4}{\text{TeV}^2} , \quad (2)$$

with a coupling constant (g) between the DM and SM particles. Therefore, if the coupling constant is of the order of the electroweak gauge couplings, dark matter physics is controlled by the TeV scale.

Motivated by the fact above, we study a simple extension of the SM at the TeV scale that incorporates a DM particle and its interaction with SM particles. In this paper, we try to extend the SM as minimally as possible. Models for DM have often been associated with solutions to the gauge hierarchy problem, a well-known example of which is the neutralino DM scenario in minimal supersymmetric standard model. However, the ATLAS and the CMS experiments searching for supersymmetric particles at the Large Hadron Collider (LHC) have been reporting negative results in all channels, that might cast doubts on the notion of naturalness and the validity of the gauge hierarchy problem. In this paper, we adopt the “minimality” as the guiding principle for model-building, instead of the naturalness of the electroweak scale.

The simplest renormalizable extension of SM that incorporates a DM particle is the so-called Higgs portal model [2], where a SM gauge singlet scalar is introduced as a DM particle and it interacts only with the Higgs boson through a renormalizable term. Unfortunately, this model is in tension with XENON 100 direct DM detection experiment [3], except for limited parameter regions where the DM mass is very close to half of the Higgs boson mass, or the DM mass is larger than about 200 GeV [4]. Although the Higgs portal dark matter might be discovered by future direct DM search experiments, the current allowed region is virtually impossible to test at collider experiments [4]; when the DM mass is larger than half of the

Higgs boson mass, the DM particles are produced only through off-shell Higgs boson and the production cross section is extremely small. The DM particles are produced through the Higgs boson decay when the DM mass is smaller than half of the Higgs boson mass. In the allowed region, however, the coupling constant among Higgs bosons and DM particles are so small that the branching ratio of the invisible Higgs decay is too tiny to observe.

Here we consider the second simplest renormalizable extension of the SM with a fermionic DM particle. In this model, we introduce a SM gauge singlet fermion (χ) and a scalar (S) charged under SM gauge groups. Odd Z_2 parity is assigned to S and χ , whereas even parity is assigned to all the SM particles. Hence, assuming χ is lighter than S , the lightest Z_2 odd particle, χ , is stable and a DM candidate. S and χ can interact with SM particles through the following renormalizable term:

$$\mathcal{L} \supset -y_i \bar{\psi}_i S \chi + \text{h.c.} , \quad (3)$$

where ψ_i denotes a SM particle with flavor index i that has the same SM charge as S . If the coupling constant y_i is of the order of the electroweak gauge couplings, then the measured DM abundance in Eq. (1) implies that the particles, χ and S , have the mass of order 100 GeV–1 TeV. There is a variety of choices for the charge assignment of S to allow the interaction in Eq. (3). In this paper, we consider the case that S is color-singlet and has the mass below 400 GeV, and the mass difference between S and χ are smaller than 50 GeV. Such a parameter choice is interesting because the charged scalar S has rich phenomenological implications, especially on the branching ratio of the Higgs boson into diphoton, but it will take time for the LHC experiments to exclude or discover the existence of the scalar and DM particles.

The heart of this study lies in the fact that since S is a scalar particle, no symmetry forbids the following renormalizable term:

$$\mathcal{L} \supset -\kappa(S^\dagger S)(H^\dagger H) , \quad (4)$$

where H is the Higgs boson in the SM. This term induces at the one-loop level an interaction between χ and SM quarks mediated by the Higgs boson and the spin-independent cross section of χ -nucleus elastic scatterings can be accessible by future direct DM detection experiments. On the other hand, since S has an electric charge and a mass less than several 100 GeV, the same term contributes to the Higgs boson decay to diphoton through a loop diagram, altering the Higgs-to-diphoton branching ratio from its SM prediction. Our model thus predicts both a signal in direct DM detection experiments and a deviation of the Higgs-to-diphoton branching ratio.

Another important result of this study is that if the DM particle is a Dirac fermion, the magnetic dipole moment of the DM particle is induced at the one-loop level. This interaction

Field	$SU(2)_L$	$U(1)_Y$	Z_2
e_{Ri}	1	-1	$+$
H	2	$-1/2$	$+$
χ	1	0	$-$
S	1	-1	$-$

Table 1: The field content of the model

gives a dominant contribution to the DM-nucleus elastic scatterings. We will find that the spin-independent cross section for the processes is below the current experimental bounds but within the reach of future experiments.

This paper is organized as follows. In the next section, we define our model. In Sec. 3, we investigate DM physics with our model. By calculating the relic abundance of the DM particle and comparing our results to the observations, we identify allowed parameter regions of the model. We also calculate the spin-independent cross section for the elastic scatterings between the DM particle and nucleus mediated by the Higgs boson. In Sec. 4, the effect of the charged scalar, S , on the Higgs branching ratio to diphoton is calculated. Then, in Sec. 5, we show correlations between the DM-nucleus elastic scattering cross section and the Higgs-to-diphoton branching ratio. Finally in Sec. 6, we discuss the case for a Dirac fermion DM particle and investigate its phenomenology.

2 Simple model for Majorana fermion dark matter

We consider a simple renormalizable extension of the SM which incorporates a fermionic DM particle interacting with SM particles. We introduce a SM gauge singlet Majorana fermion (χ) and a complex scalar field (S) with a hypercharge $Y = -1$. Odd-parity is assigned to χ and S , while even-parity to all the SM fields. The renormalizable terms involving χ and S are the following:

$$\begin{aligned}
\mathcal{L}_{extra} = & \frac{i}{2} \bar{\chi} \gamma^\mu \partial_\mu \chi - \frac{1}{2} m_\chi \bar{\chi} \chi + (D^\mu S)^\dagger (D_\mu S) - m_0^2 S^\dagger S - \lambda_S (S^\dagger S)^2 \\
& - y_i \bar{e}_{iR} S \chi + \text{h.c.} - \kappa (S^\dagger S) (H^\dagger H) ,
\end{aligned} \tag{5}$$

where e_{Ri} denotes the SM $SU(2)_L$ singlet charged lepton with flavor index i , H denotes the SM Higgs doublet field, and y_i and κ are dimensionless couplings between the new particles and the SM fields. The field contents are summarized in Table 1. The DM particle χ is assumed to be lighter than S , so that χ is stable due to the Z_2 parity and can be a DM candidate.

For general values of y_i 's, the term $y_i \bar{e}_{iR} S \chi$ induces flavor-changing neutral current processes,

which are severely constrained by current experimental results. Here we simply assume that y_i 's are aligned with respect to the SM lepton flavors, i.e., we set $y_i = y\delta_{ei}$, $y\delta_{\mu i}$ or $y\delta_{\tau i}$.

The masses of χ and S are, respectively, given by m_χ and $m_0^2 + \kappa v^2/2 \equiv m_S^2$, after the electroweak symmetry breaking by $\langle H \rangle = (v, 0)^T$ with $v = 174$ GeV. Our model is possibly constrained by the direct slepton search performed by the ATLAS experiment [6]. We here take $m_S > 100$ GeV and $m_S - m_\chi < 50$ GeV, so that the model safely evades the ATLAS bound as well as the LEP bound on charged sleptons [7].

3 Dark matter physics

In this section, we constrain the model parameters from the requirement that χ be a cold relic whose abundance fits with the WMAP data of Eq. (1). We then calculate the cross section for the DM-nucleus elastic scatterings and compare it with the current experimental bounds.

3.1 Relic abundance

The DM particle χ interacts with a SM charged lepton through the coupling y_i . When the temperature of the radiation-dominated Universe cools down below $T \sim m_\chi$, χ decouples from the thermal bath and its abundance freezes out. The decoupling process of χ is regulated by the Boltzmann equation [8]. Let s , n_χ and n_χ^{eq} , respectively, denote the entropy density, the number density of χ and the number density if χ were to stay in thermal equilibrium. We further define the following quantities:

$$z \equiv \frac{m_\chi}{T}, \quad (6)$$

$$Y(z) \equiv \frac{n_\chi(z)}{s}, \quad (7)$$

$$Y^{\text{eq}}(z) \equiv \frac{n_\chi^{\text{eq}}(z)}{s}, \quad (8)$$

$$H(T) \equiv \sqrt{\frac{\pi^2}{90} g_*} \frac{T^2}{M_P}, \quad (9)$$

where g_* denotes the effective thermal degrees of freedom during the decoupling process of χ , and $M_P = 2.4 \times 10^{18}$ GeV is the reduced Planck mass. For $m_\chi \lesssim 300$ GeV, we have $g_* = 86.25$. For $z \gtrsim 3$, $n_\chi^{\text{eq}}(z)$ can be written as

$$n_\chi^{\text{eq}}(z) = g_\chi \frac{T m_\chi^2}{2\pi^2} K_2(z), \quad (10)$$

where $g_\chi = 2$ counts the physical degree of freedom of the Majorana fermion χ .

We consider the DM pair annihilation process $\chi \chi \rightarrow e_i \bar{e}_i$, for which the thermally averaged cross section times velocity is expressed as [9]

$$\langle \sigma v \rangle = g_\chi^2 \frac{1}{(n_\chi^{\text{eq}}(z))^2} \frac{T}{32\pi^4} \int_{4m_\chi^2}^{\infty} ds \sqrt{\frac{s}{4} - m_\chi^2} K_1\left(\frac{\sqrt{s}}{T}\right) |\mathcal{M}(s)|^2, \quad (11)$$

where $|\mathcal{M}(s)|^2$ denotes the scattering rate per co-moving volume for the process and is given by

$$\begin{aligned} |\mathcal{M}(s)|^2 &= \frac{1}{g_\chi^2} \frac{y^4}{16\pi} 4 \left\{ (m_S^2 - m_\chi^2)^2 + \frac{s}{2} m_S^2 \right\} \\ &\times \frac{\sqrt{s} \sqrt{\frac{s}{4} - m_\chi^2} \left(\frac{s}{2} - m_\chi^2 + m_S^2 \right) - \left\{ (m_S^2 - m_\chi^2)^2 + s m_S^2 \right\} \arctan\left(\frac{\sqrt{s} \sqrt{s/4 - m_\chi^2}}{s/2 - m_\chi^2 + m_S^2}\right)}{\frac{\sqrt{s}}{2} \sqrt{\frac{s}{4} - m_\chi^2} \left(\frac{s}{2} - m_\chi^2 + m_S^2 \right) \left\{ (m_S^2 - m_\chi^2)^2 + s m_S^2 \right\}}. \end{aligned} \quad (12)$$

The Boltzmann equation takes the form:

$$\frac{dY(z)}{dz} = -\frac{z \langle \sigma v \rangle s}{H(m_\chi)} (Y^2(z) - Y_{\text{eq}}^2(z)). \quad (13)$$

We numerically solve the Boltzmann equation for various values of y and m_S . In our analysis, the mass of χ is taken so as to satisfy the relations, $m_\chi = m_S - 50$ GeV and $m_\chi = m_S - 20$ GeV, for simplicity. We evaluate the relic abundance of χ as $Y(z = \infty)$. In Fig. 1, we show contour plots of the relic abundance of χ on the (m_S, y^2) -plane. Regions between two (red) lines correspond to the parameter regions where the resultant DM relic abundance fits with the observed values in Eq. (1). From Fig. 1, we can see that the mass difference between χ and S does not significantly alter the relic abundance as long as the difference is within $O(10$ GeV). For the left panel in Fig. 1, we have found that the following relation must be satisfied in order to reproduce the observed DM abundance:

$$y^2 \simeq a(m_S/\text{GeV} - 100) + b, \quad (14)$$

with

$$0.0038 \leq a \leq 0.0040, \quad 0.34 \leq b \leq 0.37. \quad (15)$$

3.2 Direct Dark Matter Detection

The DM particle χ couples to SM quarks at the one-loop level through the Feynman diagrams in Fig. 3¹. We calculate effective couplings between χ and a SM quark. The Higgs boson

¹ Since χ is a Majorana fermion, photon exchange does not contribute, as it only gives rise to a magnetic dipole moment coupling.

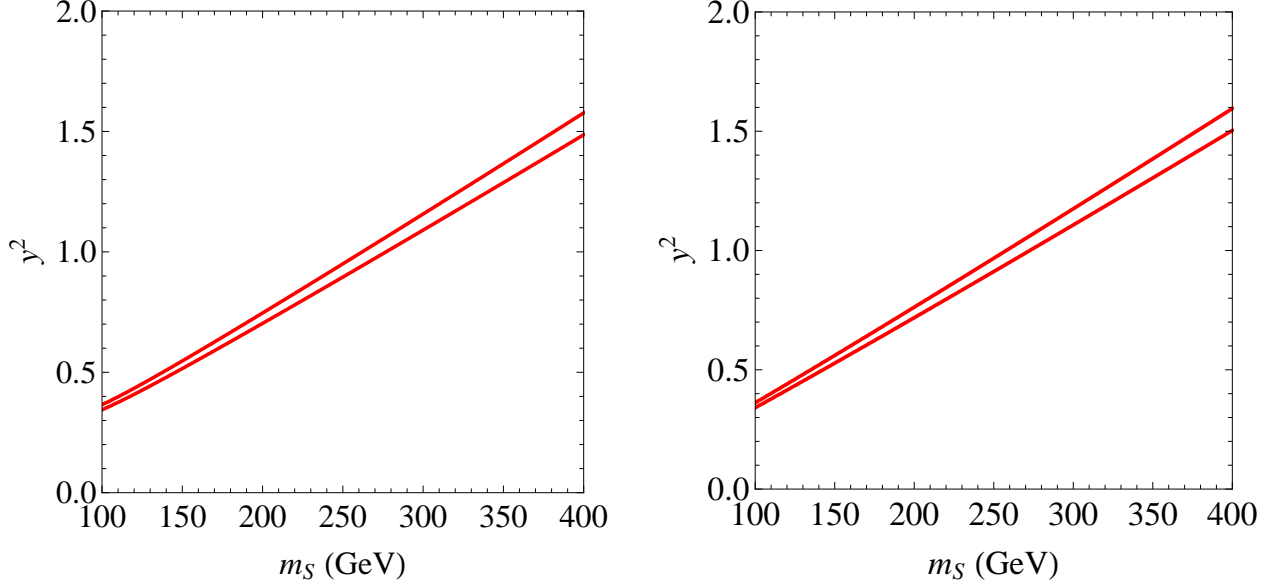


Figure 1: Contour plot for the relic abundance of the DM candidate χ on the (m_S, y^2) -plane. We have taken $m_\chi = m_S - 50$ GeV ($m_\chi = m_S - 20$ GeV) in the left (right) panel. The region between two (red) lines corresponds to the range of the observed DM abundance in Eq. (1).

exchange leads to

$$\mathcal{L}_{\text{eff}}^h = m_Q(\bar{Q}Q)(\bar{\chi}\chi) \left(\frac{-1}{16\pi^2} \right) \kappa y^2 \frac{1}{m_h^2} \frac{m_\chi}{m_S^2} \frac{x + (1-x)\ln(1-x)}{x^2}, \quad (16)$$

where Q denotes a SM quark and $x \equiv m_\chi^2/m_S^2$. An effective coupling that arises from the Z -boson exchange is given by

$$\begin{aligned} \mathcal{L}_{\text{eff}}^Z &= m_Q(\bar{Q}\gamma_5 Q)(\bar{\chi}\gamma_5 \chi) \\ &\times \frac{1}{16\pi^2} g_{Z\ell} g_{ZQ_A} y^2 \frac{1}{M_Z^2} \left(\frac{m_\chi}{m_S^2} \right) \frac{(1 - \frac{x}{3}) \ln(1-x) - x \left\{ 1 + \frac{2}{3} \ln \left(\frac{m_\ell^2}{m_S^2} \right) \right\}}{2(1-x)x}, \end{aligned} \quad (17)$$

where m_ℓ denotes the mass of the SM lepton, $g_{Z\ell}$ represents the coupling between the Z -boson and the SM lepton, and g_{ZQ_A} denotes the axial part of the coupling between Z -boson and the quark Q . In deriving Eqs. (16) and (17), we have taken the limit $m_\ell \ll m_\chi$.

Since the coupling between χ and a SM quark induced by the Z -boson exchange is of pseudo-scalar type, its contribution to DM-nucleus elastic scatterings is spin-dependent and is proportional to a DM velocity squared in the Earth frame. Therefore this contribution is negligibly small. On the other hand, the coupling induced by the Higgs boson exchange diagram is of scalar-type and hence spin-independent. This contribution to the cross section of DM-nucleus elastic scatterings can be accessible by direct DM detection experiments if a value of

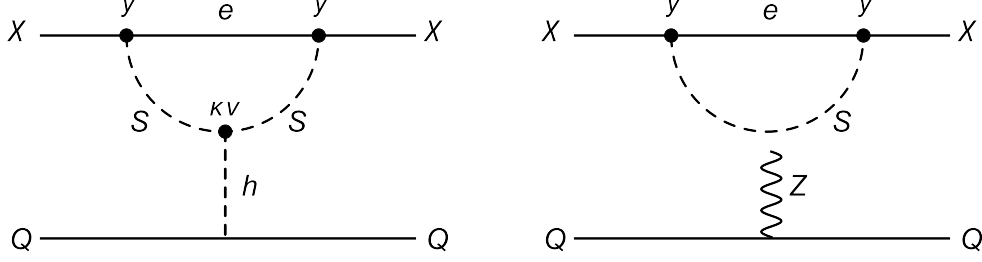


Figure 2: Feynman diagrams contributing to the interaction between χ and a SM quark. The left diagram represents the Higgs boson exchange and the right one the Z -boson exchange.

κ is large enough. In the following, we only consider the contribution from the Higgs boson exchange diagram.

Let us calculate the cross section for DM-nucleon elastic scattering. We first estimate the following matrix elements:

$$\langle N | m_Q \bar{Q} Q | N \rangle \equiv m_N f_{TQ}^N \quad (Q = u, d, s, c, b, t), \quad (18)$$

where N represents a proton, p , or a neutron, n . A recent lattice calculation [10] reports that

$$f_{Tu}^p + f_{Td}^p = f_{Tu}^n + f_{Td}^n \simeq 0.056, \quad |f_{Ts}^N| \leq 0.08. \quad (19)$$

We hereafter adopt these values, but we set $f_{Ts}^N = 0$ to make our analysis conservative. Operators involving heavy quarks, c, b, t , give rise to an effective coupling to gluons through a triangle diagram [11], and in heavy quark limit we have

$$\langle N | m_Q \bar{Q} Q | N \rangle \simeq \langle N | \left(-\frac{1}{12\pi} \alpha_s \right) G_{\mu\nu} G^{\mu\nu} | N \rangle \quad \text{for } Q = c, b, t. \quad (20)$$

Using the trace of the QCD energy momentum tensor given by

$$\theta_\mu^\mu = \sum_{Q=u,d,s,c,b,t} m_Q \bar{Q} Q - \frac{7\alpha_s}{8\pi} G_{\mu\nu} G^{\mu\nu} \simeq \sum_{Q=u,d,s} m_Q \bar{Q} Q - \frac{9\alpha_s}{8\pi} G_{\mu\nu} G^{\mu\nu}, \quad (21)$$

we obtain

$$m_N \simeq \langle N | \sum_{Q=u,d,s} m_Q \bar{Q} Q | N \rangle + \langle N | \left(\frac{-9\alpha_s}{8\pi} \right) G_{\mu\nu} G^{\mu\nu} | N \rangle. \quad (22)$$

We thus find for $Q = c, b, t$,

$$\begin{aligned} \langle N | m_Q \bar{Q} Q | N \rangle &\simeq \langle N | \left(\frac{-2\alpha_s}{24\pi} \right) G_{\mu\nu} G^{\mu\nu} | N \rangle \\ &\simeq \frac{2}{27} (1 - f_{Tu}^N - f_{Td}^N - f_{Ts}^N) m_N. \end{aligned} \quad (23)$$

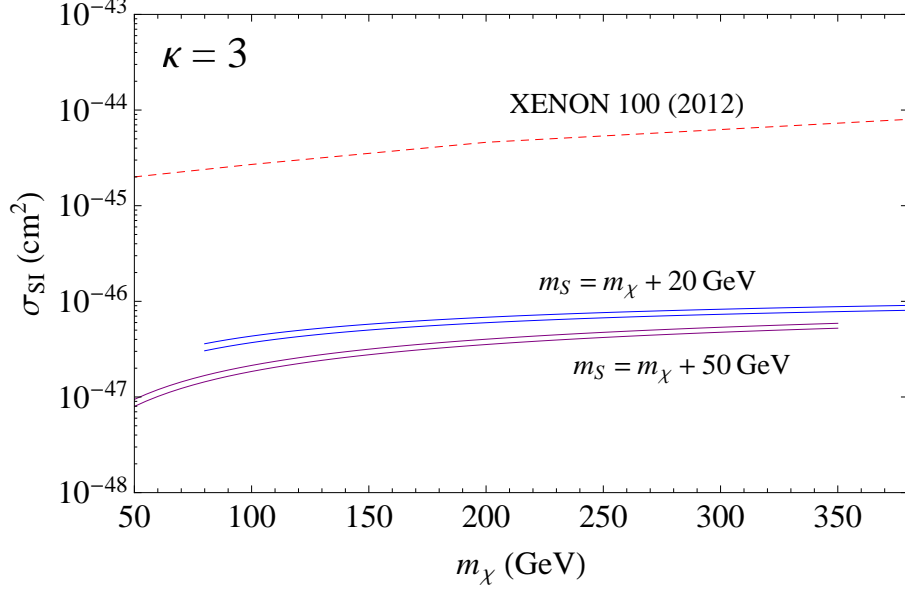


Figure 3: The spin-independent cross section for DM-nucleon elastic scattering as a function of the DM mass, m_χ . Here we have fixed $\kappa = 3$. The charged scalar mass, m_S , is related to the DM mass as $m_\chi = m_S - 50$ GeV (lower two solid lines) and $m_\chi = m_S - 20$ GeV (upper two solid lines), respectively. The coupling constant y is taken to satisfy the relation of Eq. (32) so that the model reproduces the observed DM abundance. For each pair of degenerate lines, the upper one corresponds to $(a = 0.0040, b = 0.37)$, while the lower one to $(a = 0.0038, b = 0.34)$ in eq. (14). The current experimental bound reported by the XENON 100 experiment [3] is shown by the dashed line.

Using above expressions, the spin-independent cross section for the elastic scattering of χ with a nucleon is given by

$$\begin{aligned} \sigma_{\text{SI}} &= \frac{1}{\pi} \frac{m_N^2 m_\chi^2}{(m_N + m_\chi)^2} m_N^2 \left\{ f_{Tu}^N + f_{Td}^N + f_{Ts}^N + \frac{2}{9}(1 - f_{Tu}^N - f_{Td}^N - f_{Ts}^N) \right\}^2 \\ &\times \left\{ \frac{1}{16\pi^2} \kappa y^2 \frac{1}{m_h^2} \frac{m_\chi}{m_S^2} \frac{x + (1-x)\ln(1-x)}{x^2} \right\}^2, \end{aligned} \quad (24)$$

where $m_N \simeq 1$ GeV is the mass of a nucleon (proton or neutron), and $x = m_\chi^2/m_S^2$.

We evaluate σ_{SI} for various values of $m_\chi = m_S - 50$ GeV and $m_\chi = m_S - 20$ GeV, respectively. Here, y is given as a function of m_S by using Eq. (14) so as to reproduce the observed dark matter relic abundance, and we fix the Higgs boson mass as $m_h = 125$ GeV. In Fig. 3, we show σ_{SI} as a function of m_χ for $\kappa = 3$, along with the current upper bound reported by the XENON 100 experiment [3]. The resultant cross section is found to be (far) below the upper bound. Note that σ_{SI} scales as κ^2 . If we allow a value of $|\kappa|$ as large as its naive upper bound, $|\kappa| \leq 4\pi$, from the view point of perturbation theory, the spin-independent cross section can be close

to the current limit. The sensitivity of the spin-independent cross section in the future direct DM detection experiments, such as the XENON 1T [12], is expected to reach $(2 - 8) \times 10^{-47} \text{ cm}^{-2}$, and hence our scenario can be tested. As we will discuss in the next sections, the spin-independent cross section has a correlation with a deviation of the Higgs-to-diphoton branching ratio from the SM predicted value. We will see that the deviation becomes larger as $|\kappa|$ is raised, equivalently, the spin-independent cross section becomes larger.

4 Anomalous Higgs coupling to diphoton

Although the Higgs boson discovered at the LHC experiments [5] has shown its properties mostly consistent with those expected in the SM, there exist some deviations from the SM expectations, namely, in its signal strength of the diphoton decay mode. Since the Higgs-to-diphoton coupling arises at the quantum level even in the SM, there is a good chance for certain new physics effects to alter the coupling. This has motivated many recent studies [13, 14]. For studies in this direction before the Higgs boson discovery, see, for example, [15].

In our model, the charged scalar S couples to the Higgs boson through the term:

$$\mathcal{L} \supset -\kappa(S^\dagger S)(H^\dagger H). \quad (25)$$

Hence a one-loop diagram involving S gives a new contribution to the effective Higgs-to-diphoton coupling. The amplitude of the loop diagram of S is given by [16]

$$\mathcal{A}_S = C \kappa \frac{v^2}{m_S^2} \frac{1}{x_S^2} [-x_S + f(x_S)] , \quad (26)$$

while the amplitudes in the SM via the top quark loop and the W -boson loop are, respectively, given by

$$\mathcal{A}_t = C N_c Q_f^2 \frac{2}{x_t^2} [x_t + (x_t - 1)f(x_t)] , \quad (27)$$

$$\mathcal{A}_W = -C \frac{1}{x_W^2} [2x_W^2 + 3x_W + 3(2x_W - 1)f(x_W)] , \quad (28)$$

where C is a common constant, $v = 174 \text{ GeV}$, $N_c = 3$, $Q_f = 2/3$, $x_S \equiv m_h^2/4m_S^2$, $x_t \equiv m_h^2/4m_t^2$, and $x_W \equiv m_h^2/4m_W^2$. The function $f(x)$ is defined as

$$f(x) \equiv \arcsin^2(\sqrt{x}) \quad (29)$$

for $x > 1$.

We define the ratio of the branching fraction $\text{Br}(h \rightarrow \gamma\gamma)$ over its SM value as

$$r_{\gamma\gamma} \equiv \frac{\text{Br}(h \rightarrow \gamma\gamma)}{\text{Br}(h \rightarrow \gamma\gamma)|_{\text{SM}}} = \left| 1 + \frac{\mathcal{A}_S}{\mathcal{A}_t + \mathcal{A}_W} \right|^2 . \quad (30)$$

Note that as long as $|\mathcal{A}_S| < |\mathcal{A}_t + \mathcal{A}_W|$, \mathcal{A}_S interferes constructively (destructively) with the SM contributions when $\kappa > 0$ ($\kappa < 0$). If $|\kappa|$ is large and/or the scalar S is light, $|\mathcal{A}_S|$ can cause a sizable deviation of the ratio from the SM prediction $r_{\gamma\gamma} = 1$.

5 Implications to future experiments

In our analysis, only three parameters (y , κ and m_S) are involved with the fixed mass difference of $m_\chi = m_S - 50$ GeV or $m_\chi = m_S - 20$ GeV. In order to reproduce the measured relic abundance, we have found the relation between y and m_S in Eq. (14), by which only two parameters (κ and m_S) are left free. As a result, both the spin-independent cross section in Eq. (24) and the ratio of the Higgs-to-diphoton branching ratio in Eq. (30) can be obtained as a function of the two free parameters. Therefore, for a fixed m_S value, there is a correlation between σ_{IS} and $r_{\gamma\gamma}$ through κ .

Fig. 4 shows the correlation for various values of m_S with the fixed mass difference of $m_\chi = m_S - 50$ GeV. As $|\kappa|$ is raised, the resultant spin-independent cross section increases and the deviation of $r_{\gamma\gamma}$ from the SM value $r_{\gamma\gamma} = 1$ becomes larger. In the Figure, we have imposed the condition $|\kappa| < 4\pi$ as a naive perturbative bound, which gives the upper bound on the cross section and the deviation of $r_{\gamma\gamma}$ for a fixed m_S value. We have found that in order for the spin-independent cross section to be within the reach of the future experimental sensitivity $\sigma_{\text{IS}} \gtrsim 10^{-47} \text{ cm}^2$, the deviation of $r_{\gamma\gamma}$ from the SM prediction should remain sizable. Therefore, the precise measurement of Higgs boson decay to diphoton at the LHC and the future direct DM detection experiments are complementary to reveal our scenario.

6 Case for Dirac fermion dark matter

In general, we can also consider a model similar to the one described in Sec. 2 except that χ is a Dirac fermion (see [17] for a similar model). In this case, we introduce a global U(1) symmetry, instead of the Z_2 parity in Table 1. We may assign U(1) charge +1 (−1) for the Dirac fermion DM (the complex scalar χ). The basic Lagrangian remains the same as Eq. (5) (except for the correct normalization factor for the Dirac fermion). In this section, we will investigate phenomenology for the Dirac fermion case.

Let us first evaluate the relic abundance of χ in the same way as in Subsection 2.1 but for

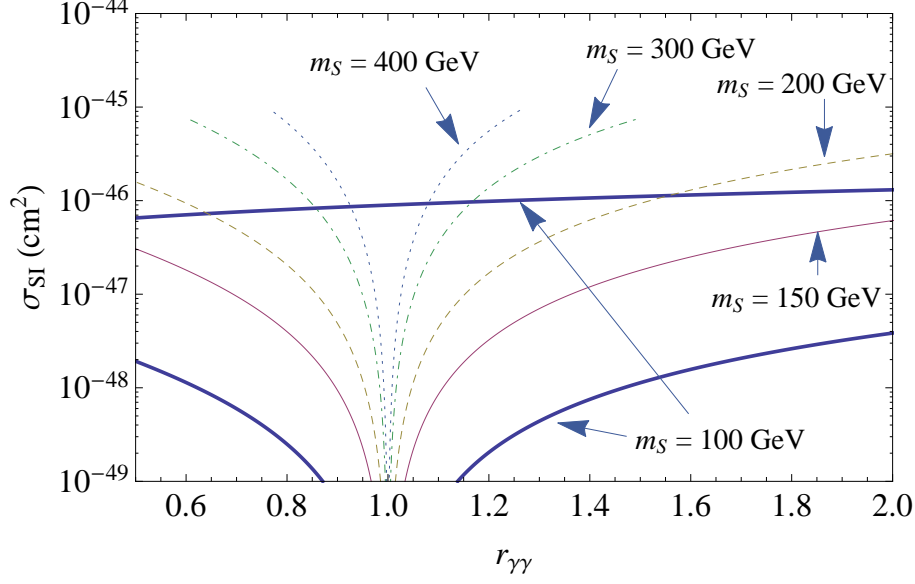


Figure 4: Correlation between $r_{\gamma\gamma}$ and σ_{SI} through $|\kappa| < 4\pi$ with various m_S values. The thick solid line, thin solid line, dashed line, dot-dashed line and dotted line, respectively, correspond to the charged scalar mass of $m_S = 100$ GeV, 150 GeV, 200 GeV, 300 GeV and 400 GeV. The DM mass, m_χ , is taken as $m_\chi = m_S - 50$ GeV.

the Dirac fermion, $|\mathcal{M}(s)|^2$ is replaced by

$$\begin{aligned}
|\mathcal{M}(s)|^2 &= \frac{1}{g_\chi^2} \frac{y^4}{16\pi} 4 \frac{1}{2\sqrt{s-4m_\chi^2}\sqrt{s}} \\
&\times \left\{ \frac{(m_\chi^2 - m_S^2)^2}{m_\chi^2 - m_S^2 - \frac{1}{2}(s + \sqrt{s-4m_\chi^2}\sqrt{s})} - \frac{(m_\chi^2 - m_S^2)^2}{m_\chi^2 - m_S^2 - \frac{1}{2}(s - \sqrt{s-4m_\chi^2}\sqrt{s})} \right. \\
&+ \left. 2(m_\chi^2 - m_S^2) \log \left[\frac{m_S^2 - m_\chi^2 + \frac{1}{2}(s + \sqrt{s-4m_\chi^2}\sqrt{s})}{m_S^2 - m_\chi^2 + \frac{1}{2}(s - \sqrt{s-4m_\chi^2}\sqrt{s})} \right] + \sqrt{s-m_\chi^2}\sqrt{s} \right\}, \quad (31)
\end{aligned}$$

with $g_\chi = 4$. Numerically solving the Boltzmann equation, we find the DM relic abundance as a function of m_S and y^2 . Corresponding to Fig. 1, we show our result in Fig. 5, for $m_\chi = m_S - 50$ GeV. As in the case of Majorana fermion DM, the difference between m_χ and m_S does not significantly alter our results as long as the difference is within $O(10)$ GeV. From Fig. 5, we find that the relation

$$y^2 \simeq a(m_S/\text{GeV} - 100) + b \quad (32)$$

with

$$0.0025 \leq a \leq 0.0027, \quad 0.29 \leq b \leq 0.31, \quad (33)$$

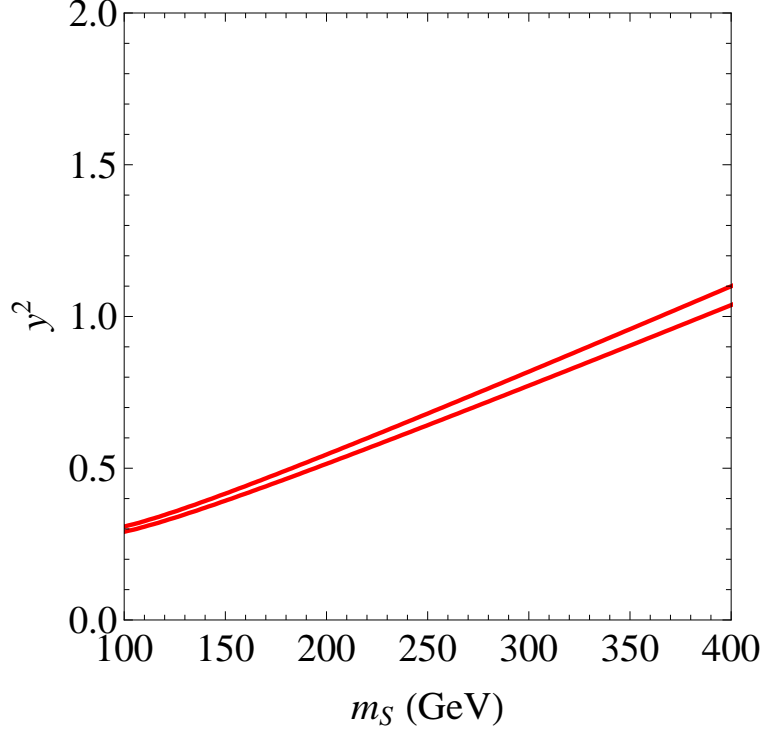


Figure 5: Contour plot for the relic abundance of the DM candidate χ on the (m_S, y^2) -plane. Here we have taken $m_\chi = m_S - 50$ GeV. The region between two (red) lines corresponds to the range of the observed DM abundance in Eq. (1).

in order to reproduce the range of the observed relic abundance in Eq. (1).

As in the Majorana case, the DM couples to SM quarks at the one-loop level. In addition to the diagrams in Fig. 2, there is a diagram mediated by photon, shown in Fig. 6, through the magnetic dipole moment induced at one-loop level. In fact, this new diagram gives a dominant contribution to the spin-independent cross section for the DM elastic scattering with nucleus². The effective coupling induced by the magnetic dipole moment is found to be

$$\mathcal{L}_{\text{eff}} = (\bar{Q}\gamma^\mu Q)(\bar{\chi}\sigma_{\mu\nu}q^\nu\chi) \times \left(\frac{-1}{16\pi^2}\right) g_{\gamma Q} g_{\gamma l} y^2 \frac{1}{q^2} \frac{m_\chi}{m_S^2} \frac{x + \log(1-x)}{2x^2}, \quad (34)$$

where q^μ denotes the momentum transfer from χ to a quark (Q), $g_{\gamma l}$ ($g_{\gamma Q}$) denotes the QED coupling of the SM lepton (the SM quark), and $x \equiv m_\chi^2/m_S^2$.

The effective charge-charge coupling induced at one-loop level is found to be

Since the vector interactions with each quarks coherently contribute to the total cross section, we obtain the differential cross section for χ -nucleus elastic scattering (in the center-of-

² For general discussions for a DM particle with electric/magnetic dipole moments, see Ref. [18].

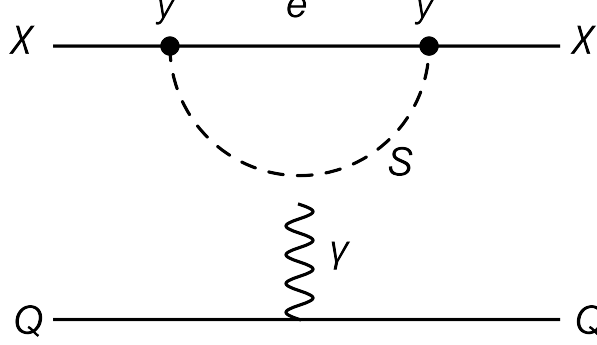


Figure 6: Feynman diagram that gives a dominant contribution to the interaction between χ and a SM quark when χ is a Dirac fermion.

mass frame) as

$$\frac{d\sigma_{\chi-NS}}{d(\cos\theta)} = \frac{1}{8\pi} (Ze)^2 g_{\gamma l}^2 \left[\frac{2}{1 - \cos\theta} + \frac{m_\chi^2 - 2m_{NS}m_\chi}{(m_{NS} + m_\chi)^2} \right] \left[\frac{y^2}{16\pi^2} \frac{m_\chi}{m_S^2} \frac{x + \log(1-x)}{2x^2} \right]^2, \quad (35)$$

where m_N and Z respectively denote the mass and the atomic number of a nucleus. The divergence at $\theta = 0$ is cut off by the low energy threshold for a recoiling nucleus. To make a conservative comparison of the cross section in our model with the bounds reported by direct DM detection experiments³, we replace $\cos\theta \rightarrow -1$ in the right hand side of Eq. (35). Then the conservatively-estimated total cross section for χ -nucleus elastic scattering is given by

$$\begin{aligned} \bar{\sigma}_{\chi-NS} &= \int_{-1}^1 d\cos\theta \frac{d\sigma_{\chi-nucleus}}{d(\cos\theta)} \Big|_{\cos\theta=-1} \\ &= \frac{1}{4\pi} (Ze)^2 g_{\gamma l}^2 \left[1 + \frac{-2m_{NS}m_\chi + m_\chi^2}{(m_{NS} + m_\chi)^2} \right] \left[\frac{1}{16\pi^2} y^2 \frac{m_\chi}{m_S^2} \frac{x + \log(1-x)}{2x^2} \right]^2. \end{aligned} \quad (36)$$

We finally translate the DM-nucleus elastic scattering cross section into the spin-independent cross section for DM-nucleon elastic scattering, (σ_{SI}) as follows:

$$\sigma_{SI} = \bar{\sigma}_{\chi-NS} \times \frac{m_N^2}{m_{NS}^2} \frac{(m_{NS} + m_\chi)^2}{(m_N + m_\chi)^2} \frac{1}{A^2}, \quad (37)$$

³ Direct DM detection experiments actually put a bound on the normalization for the distribution of the event rate per recoil energy, dR/dE_r (R denotes the event rate and E_r the recoil energy), with the assumption that $dR/dE_r \propto \exp(-AE_r)$, where A is some known constant. In our case, however, we have $dR/dE_r \propto (1 + B/E_r) \exp(-AE_r)$ with a constant B because of the term $1/(1 - \cos\theta)$ in Eq. (35). Thus, we cannot naively compare the elastic scattering cross section in our model with an experimental bound. All we can do is to make a conservative estimate on the cross section by substituting -1 into $\cos\theta$, and compare it with the experimental bound.

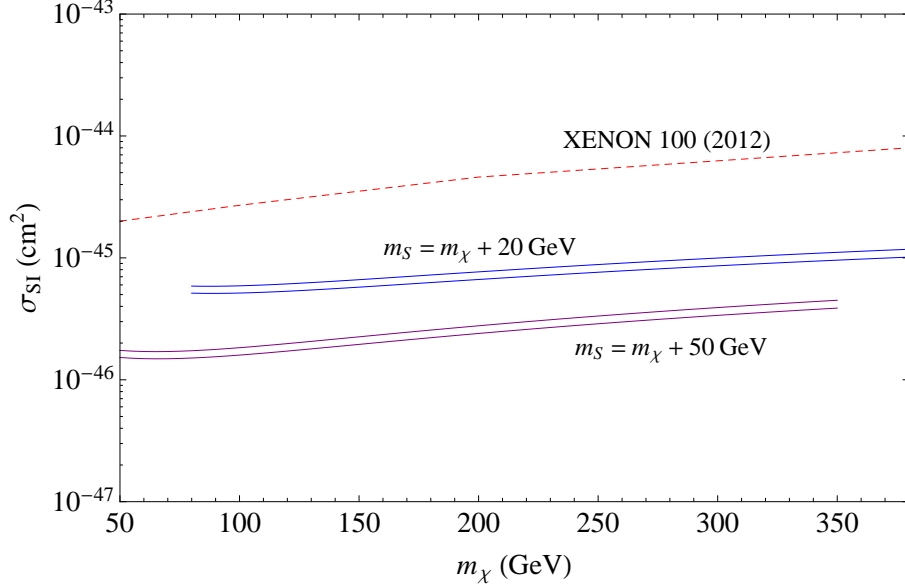


Figure 7: The conservatively-estimated spin-independent cross section for DM-nucleon elastic scattering (σ_{SI}) as a function of the DM mass (m_χ). The charged scalar mass, m_S , is related to the DM mass as $m_\chi = m_S - 50$ GeV (lower two solid lines) and $m_\chi = m_S - 20$ GeV (upper two solid lines). The coupling constant y is taken to satisfy the relation in Eq. (32) so that the model reproduces the observed DM abundance. For each pair of degenerate solid lines, the upper line corresponds to $(a = 0.0027, b = 0.31)$ in Eq. (32), while the lower one to $(a = 0.0025, b = 0.29)$. For comparison, the current experimental bound reported by the XENON 100 experiment [3] is shown by the dashed line.

where A denotes the mass number of the nucleus. For the XENON 100 experiment, we take $Z = 54$ and $A = 131.3$.

In Fig. 7, we show the conservatively-estimated spin-independent cross section for χ -nucleon elastic scattering, σ_{SI} , as a function of m_χ which is taken to be $m_\chi = m_S - 50$ GeV and $m_\chi = m_S - 20$ GeV, respectively. Here, y is fixed to satisfy the relation of Eq. (32). We see that the resultant cross sections are about an order of magnitude smaller than the current upper bound and will be tested in future direct DM detection experiments.

Acknowledgments

This work is supported in part by the DOE Grant No. DE-FG02-10ER41714 (N.O.), and by the grant of the Japan Society for the Promotion of Science, No. 23-3599 (T.Y.).

References

- [1] N. Jarosik *et al.*, *Astrophys. J. Supp.* **192** (2011) 14; D. Larson *et al.*, *Astrophys. J. Supp.* **192** (2011) 16; E. Komatsu *et al.*, *Astrophys. J. Supp.* **192** (2011) 18.
- [2] J. McDonald, *Phys. Rev. D* **50**, 3637 (1994); C. P. Burgess, M. Pospelov and T. ter Veldhuis, *Nucl. Phys. B* **619**, 709 (2001).
- [3] E. Aprile *et al.* [XENON100 Collaboration], *Phys. Rev. Lett.* **109**, 181301 (2012).
- [4] See, for example, S. Kanemura, S. Matsumoto, T. Nabeshima and N. Okada, *Phys. Rev. D* **82** (2010) 055026; Y. Mambrini, *Phys. Rev. D* **84** (2011) 115017, and references therein.
- [5] G. Aad *et al.* (ATLAS Collaboration), *Phys. Lett. B* **716** (2012) 1; S. Chatrchyan *et al.* (CMS Collaboration), *Phys. Lett. B* **716** (2012) 30.
- [6] G. Aad *et al.* [ATLAS Collaboration], *Phys. Lett. B* **718**, 879 (2013).
- [7] LEP SUSY Working Group (ALEPH, DELPHI, L3, OPAL), Notes LEPSUSYWG/01-03.1 and 04-01.1, <http://lepsusy.web.cern.ch/lepsusy/Welcome.html>.
- [8] See, e.g., E. W. Kolb, and M. S. Turner, *The Early Universe* (Addison-Wesley).
- [9] J. Edsjo and P. Gondolo, *Phys. Rev. D* **56** (1997) 1879.
- [10] H. Ohki *et al.*, *Phys. Rev. D* **78** (2008) 054502.
- [11] R. Crewther, *Phys. Rev. Lett.* **28** (1972) 1421; M. Chanowitz and J. Ellis, *Phys. Lett.* **40B** (1972) 397; *Phys. Rev. D* **7** (1973) 2490; J. Collins, L. Duncan and S. Joglekar, *Phys. Rev. D* **16** (1977) 438; M. A. Shifman, A. I. Vainshtein and V. I. Zakharov, *Phys. Lett. B* **78** (1978) 443.
- [12] E. Aprile [XENON1T Collaboration], arXiv:1206.6288 [astro-ph.IM].
- [13] M. Carena, S. Gori, N. R. Shah and C. E. M. Wagner, *JHEP* **1203**, 014 (2012); *JHEP* **1302**, 114 (2013); J. -J. Cao, Z. -X. Heng, J. M. Yang, Y. -M. Zhang and J. -Y. Zhu, *JHEP* **1203**, 086 (2012); M. Carena, S. Gori, N. R. Shah, C. E. M. Wagner and L. -T. Wang, *JHEP* **1207**, 175 (2012); H. An, T. Liu and L. -T. Wang, *Phys. Rev. D* **86**, 075030 (2012); N. Haba, K. Kaneta, Y. Mimura and R. Takahashi, *Phys. Lett. B* **718**, 1441 (2013); M. A. Ajaib, I. Gogoladze and Q. Shafi, *Phys. Rev. D* **86**, 095028 (2012); K. Schmidt-Hoberg and F. Staub, *JHEP* **1210**, 195 (2012); R. Sato, K. Tobioka and N. Yokozaki, *Phys.*

- Lett. B **716**, 441 (2012); T. Kitahara, JHEP **1211**, 021 (2012); M. Berg, I. Buchberger, D. M. Ghilencea and C. Petersson, arXiv:1212.5009 [hep-ph].
- [14] B. Batell, S. Gori and L. -T. Wang, JHEP **1206**, 172 (2012); S. Kanemura and K. Yagyu, Phys. Rev. D **85**, 115009 (2012); A. G. Akeroyd and S. Moretti, Phys. Rev. D **86**, 035015 (2012); W. -F. Chang, J. N. Ng and J. M. S. Wu, Phys. Rev. D **86**, 033003 (2012); M. Carena, I. Low and C. E. M. Wagner, JHEP **1208**, 060 (2012); A. Alves, A. G. Dias, E. R. Barreto, C. A. de S. Pires, F. S. Queiroz and P. S. R. da Silva, arXiv:1207.3699 [hep-ph]; T. Abe, N. Chen and H. -J. He, JHEP **1301**, 082 (2013); A. Joglekar, P. Schwaller and C. E. M. Wagner, JHEP **1212**, 064 (2012); N. Arkani-Hamed, K. Blum, R. T. D’Agnolo and J. Fan, arXiv:1207.4482 [hep-ph]; L. G. Almeida, E. Bertuzzo, P. A. N. Machado and R. Z. Funchal, JHEP **1211**, 085 (2012); M. Hashimoto and V. A. Miransky, Phys. Rev. D **86**, 095018 (2012); M. Reece, arXiv:1208.1765 [hep-ph]; H. Davoudiasl, H. -S. Lee and W. J. Marciano, Phys. Rev. D **86**, 095009 (2012); M. B. Voloshin, Phys. Rev. D **86**, 093016 (2012); A. Kobakhidze, arXiv:1208.5180 [hep-ph]; A. Urbano, arXiv:1208.5782 [hep-ph]; L. Wang and X. -F. Han, Phys. Rev. D **87**, 015015 (2013); E. J. Chun, H. M. Lee and P. Sharma, JHEP **1211**, 106 (2012); H. M. Lee, M. Park and W. -I. Park, JHEP **1212**, 037 (2012); L. Wang and X. -F. Han, arXiv:1209.0376 [hep-ph]; B. Batell, S. Gori and L. -T. Wang, arXiv:1209.6382 [hep-ph]; M. Chala, arXiv:1210.6208 [hep-ph]; B. Batell, S. Jung and H. M. Lee, arXiv:1211.2449 [hep-ph]; C. -W. Chiang and K. Yagyu, arXiv:1211.2658 [hep-ph]; H. Davoudiasl, I. Lewis and E. Ponton, arXiv:1211.3449 [hep-ph]; M. Aoki, S. Kanemura, M. Kikuchi and K. Yagyu, arXiv:1211.6029 [hep-ph]; F. Arbabi-ar, S. Bahrami and M. Frank, arXiv:1211.6797 [hep-ph]; S. Funatsu, H. Hatanaka, Y. Hosotani, Y. Orikasa and T. Shimotani, arXiv:1301.1744 [hep-ph]; P. S. B. Dev, D. K. Ghosh, N. Okada and I. Saha, JHEP **1303**, 150 (2013). N. Maru and N. Okada, arXiv:1303.5810 [hep-ph]; A. Carmona and F. Goertz, arXiv:1301.5856 [hep-ph].
- [15] F. J. Petriello, JHEP **0205**, 003 (2002); S. K. Rai, Int. J. Mod. Phys. A **23**, 823 (2008); C. -R. Chen, K. Tobe and C. -P. Yuan, Phys. Lett. B **640**, 263 (2006); R. Dermisek and I. Low, Phys. Rev. D **77**, 035012 (2008); T. Kikuchi and N. Okada, Phys. Lett. B **661**, 360 (2008); A. Falkowski, Phys. Rev. D **77**, 055018 (2008); N. Maru and N. Okada, Phys. Rev. D **77**, 055010 (2008); I. Low, R. Rattazzi and A. Vichi, JHEP **1004**, 126 (2010).
- [16] M. A. Shifman, A. Vainshtein, M. Voloshin and V. I. Zakharov, Sov. J. Nucl. Phys. **30** (1979) 711; G. K. S. D. John, F. Gunion and H. E. Haber, *The Higgs Hunters Guide* (Westview Press).
- [17] P. Agrawal, S. Blanchet, Z. Chacko and C. Kilic, Phys. Rev. D **86**, 055002 (2012).

- [18] K. Sigurdson, M. Doran, A. Kurylov, R. R. Caldwell and M. Kamionkowski, Phys. Rev. D 70 (2004) 083501, Erratum-ibid. D 73 (2006) 089903; E. Masso, S. Mohanty and S. Rao, Phys. Rev. D **80**, 036009 (2009); J. -F. Fortin and T. M. P. Tait, Phys. Rev. D **85**, 063506 (2012).